

*Physics*

*Physics Research Publications*

---

*Purdue University*

*Year 2008*

---

The TeV energy spectrum of Markarian  
421 measured in a high flaring state

A. Konopelko

W. Cui

C. Duke

J. P. Finley

This paper is posted at Purdue e-Pubs.

[http://docs.lib.purdue.edu/physics\\_articles/656](http://docs.lib.purdue.edu/physics_articles/656)

## THE TeV ENERGY SPECTRUM OF MARKARIAN 421 MEASURED IN A HIGH FLARING STATE

ALEXANDER KONOPELKO,<sup>1</sup> WEI CUI,<sup>1</sup> CHARLIE DUKE,<sup>2</sup> AND JOHN P. FINLEY<sup>1</sup>

*Received 2008 February 18; accepted 2008 April 4; published 2008 April 29*

### ABSTRACT

The BL Lac object (blazar) Mrk 421 was observed during its outburst in 2004 April with the Whipple 10 m telescope for a total of about 24.5 hr. The measured  $\gamma$ -ray rate varied substantially over the range from 4 to 10  $\text{minute}^{-1}$  and eventually exceeded the steady  $\gamma$ -ray rate of the Crab Nebula (standard candle) by a factor of 3. The overall significance of the  $\gamma$ -ray signal exceeded  $70\sigma$  and the total number of excess events was more than 10,000. This unique Mrk 421 outburst enabled the measurement of a high-quality spectrum of very high energy  $\gamma$ -rays in a high state of emission. This spectrum is a power law and it extends beyond 10 TeV.

*Subject headings:* BL Lacertae objects: individual (Markarian 421) — galaxies: active

*Online material:* color figure

### 1. INTRODUCTION

Mrk 421 is the first detected, the closest known (redshift  $z = 0.030$ ), and one of the best studied TeV  $\gamma$ -ray emitting blazars. The very high energy (VHE)  $\gamma$ -ray emission arises from the particles accelerated in a relativistic jet directed along our line of sight. Since its discovery, Mrk 421 has shown very low baseline TeV  $\gamma$ -ray emission with a few extremely rapid flares on timescales from 1 day to 15 minutes (Gaidos et al. 1996). In 2000 and 2001 Mrk 421 went into a flare state with an average flux of 4 times that of the Crab Nebula. Data taken during this flare have been used to extract the energy spectrum at high energies, up to 20 TeV. Noticeable variations in the hardness of the TeV  $\gamma$ -ray energy spectrum have been reported (Aharonian et al. 2002; Krennrich et al. 2002). A number of successful multiwavelength campaigns for Mrk 421 have revealed evidence of a correlation of the simultaneously measured fluxes in X-ray and TeV  $\gamma$ -ray energy bands (Krawczynski et al. 2001; Blazejowski et al. 2005).

A one-zone synchrotron self-Compton (SSC) model described the observational results reasonably well (e.g., Konopelko et al. 2003). During 2004 April, an intensive multiwavelength monitoring campaign on the TeV blazar Mrk 421 was performed simultaneously in radio, optical, X-rays, and  $\gamma$ -rays. The source was seen to be active in X-rays and TeV  $\gamma$ -rays with the peak flux exceeding the 3 crab level (Blazejowski et al. 2005). The time-averaged energy spectrum of Mrk 421 during the flaring state has been measured at high energies with H.E.S.S. using large-zenith-angle observations (Aharonian et al. 2005), and with MAGIC (Albert et al. 2007). The Whipple 10 m telescope observed Mrk 421 extensively during the 2004 April flare. Here we report the results on the TeV  $\gamma$ -ray energy spectrum of Mrk 421 measured in a high flaring state during the 2004 April outburst with the Whipple 10 m telescope.

### 2. THE 10 m WHIPPLE TELESCOPE

The reflector of the Whipple Observatory imaging atmospheric Cerenkov telescope (IACT) is a tessellated structure consisting of 248 spherical mirrors, which are hexagonal in shape and 61 cm from apex to apex, arranged in a hexagonal pattern. The mirrors are mounted on a steel support structure,

which has a 7.3 m radius of curvature with a 10 m aperture. Each individual mirror has  $\sim 14.6$  m radius of curvature and is pointed toward a position along the optical axis at 14.6 m from the reflector. This arrangement constitutes a Davies-Cotton design (Davies & Cotton 1957) of the optical reflector. The point-spread function of the telescope has a FWHM of  $\sim 7.2'$  on-axis.

In 1999, a high-resolution camera (GRANITE III) was installed at the telescope (Finley et al. 2001). It consists of 379 photomultiplier tubes (PMTs) in a close packed hexagonal arrangement (each PMT subtending  $0.11^\circ$  on the sky) and has a  $2.6^\circ$  diameter. A set of light concentrators is mounted in front of the pixels to increase the light-collection efficiency by  $\sim 38\%$ . The camera triggers if the signal in each of at least 3 neighboring PMTs out of the inner 331 exceeds a threshold of 32 mV, corresponding to  $\sim 8$ – $10$  photoelectrons. The post-GRANITE III upgrade trigger rate of the Whipple Observatory 10 m telescope is  $\sim 20$ – $30$  Hz at zenith.

### 3. OBSERVATIONS AND ANALYSIS

Mrk 421 was observed with the Whipple Observatory 10 m IACT for about 24.5 hr of on-source data between 2004 April 9 and April 23. Data were taken in good weather at zenith angles of less than  $30^\circ$  (mean elevation is about  $75^\circ$ ). During observations the raw detection rate was about 22 Hz. Observations were performed using tracking mode in data runs of 28 minutes each. The recorded images are first flat-fielded using nightly measured nitrogen arc lamp PMT responses and then cleaned by applying a standard picture and boundary technique with canonical thresholds of 4.25 and 2.25 times the standard deviation of the PMT pedestal distributions, respectively (see, e.g., Kildea et al. 2008). To characterize the shape and orientation of calibrated images, the standard second-moment image parameters are calculated as described in Reynolds et al. (1993). The CAnalyze package developed at Purdue University (Lessard et al. 2001) is used for the primary data analysis. Analysis methods known as Supercuts (see Tables 1 and 2) and extended Supercuts are applied for the  $\gamma$ -ray/hadron separation. The latter utilizes dynamic, energy-dependent orientation and shape cuts. The significance map of the sky region around Mrk 421 for the data set corresponding to a high emission state (exposure of 55 minutes) is shown in Figure 1. The energy spectrum of Mrk 421 is reconstructed using algorithms described in Mohanty et al. (1998).

<sup>1</sup> Department of Physics, Purdue University, West Lafayette, IN 47907.

<sup>2</sup> Grinnell College, Department of Physics, 1116 8th Avenue, Grinnell, IA 50112-1690.

TABLE 1  
SUPERCUTS SELECTION CRITERIA FOR THE WHIPPLE  
OBSERVATORY 10 m TELESCOPE

Quantity	Image Parameter Cut
Trigger .....	First and second brightest pixel > 30 dc
Shape .....	0.05° < width < 0.12°
	0.13° < length < 0.25°
Muon cut .....	length/size < 0.0004 deg dc <sup>-1</sup>
Quality cut .....	0.4° < distance < 1.0°
Orientation .....	α < 15°

NOTE.—Here “dc” stands for digital counts.

4. SIMULATIONS

The KASCADE shower simulation code (Kertzmann & Sembroski 1994) is used for generating the  $\gamma$ -ray and cosmic-ray induced air showers within the corresponding range of zenith angles and in the primary energy range between 50 GeV and 100 TeV, assuming the  $\gamma$ -ray energy spectrum to be a power law of 2.5. Simulations of the response of the Whipple Observatory 10 m telescope are carried out using the GRISU code, developed by the Grinnell College and Iowa State University groups.

5. RESULTS

The light curve of Mrk 421, measured with the Whipple Observatory 10 m telescope during the outburst in 2004 April, does not reveal any particular pattern (Fig. 2). Two data runs with a flux above 3 crab and an exposure of 55 minutes give an exceptionally high  $\gamma$ -ray rate with an average value of 9.85 minute<sup>-1</sup> and a total of 545 excess counts. This excess corresponds to a significance of the  $\gamma$ -ray signal at a level of 16.4  $\sigma$ . This high-flux data set enabled measurements of the energy spectrum of TeV  $\gamma$ -ray emission. The corresponding  $\gamma$ -ray energy spectrum is consistent with a pure power law of index 2.66. This spectrum does not indicate any apparent gradual change of slope (see Fig. 3). Such unusual behavior of the Mrk 421 TeV  $\gamma$ -ray spectrum measured in a high emission state suggests that the previously observed curvature in the Mrk 421  $\gamma$ -ray spectrum is an intrinsic feature of the source rather than the footprint of  $\gamma$ -ray absorption by interacting with the soft photons of extragalactic background light.

6. MODELING

To model the multiwavelength spectrum of the BL Lac object Mrk 421 in a homogeneous SSC scenario we use an approach described in Mastichiadis & Kirk (1997). This method involves prescribing an injection function for relativistic electrons and solving the two time-dependent kinetic equations for the electron and photon distributions of the source. All relevant physical processes are taken into account in the code, i.e., synchrotron radiation, inverse Compton scattering, photon-photon pair production, and synchrotron self-absorption. Seven model parameters are required to specify a source in a stationary state. These are the Doppler factor  $\delta$ , the radius  $R$  of the source, the

TABLE 2  
SUMMARY OF MARKARIAN 421 DATA ANALYZED BY STANDARD SUPERCUTS  
CRITERIA (SEE TABLE 1)

Observation	Time (minutes)	ON	OFF	Excess	$R_\gamma$ (minute <sup>-1</sup> )	S/N ( $\sigma$ )
April 2004 .....	1472	18383	6872	11511	7.82	71.82
High state .....	55	825	280	545	9.85	16.40

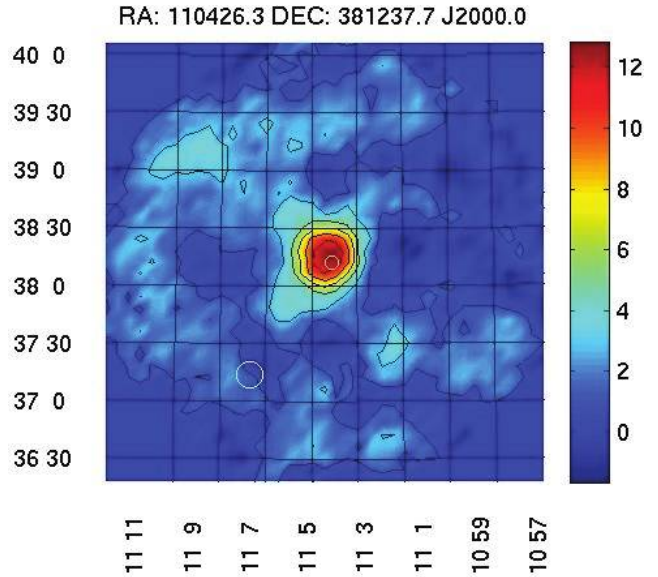


FIG. 1.—Two-dimensional map of excess significances over the sky region around Mrk 421 generated for the data sample corresponding to a high emission state. The map of uncorrelated rectangular angular bins of a 0.1° size has been smoothed using a Gaussian kernel with an angular size of  $\sigma = 0.22^\circ$ . The maximal significance of  $\gamma$ -ray excess using this analysis is 12.3  $\sigma$ .

magnetic field strength  $B$ , the index  $s$  of the electron injection spectrum, the Lorentz factor at the cutoff of the injection spectrum  $\gamma_{\max}$ , the amplitude of the injection spectrum  $q_e$ , and the effective escape time of relativistic electrons  $t_{\text{esc}}$ . To optimize a fit to a particular data set, we used physically motivated starting values for these seven parameters (see Konopelko et al. 2003). This is done by identifying six scalars characterizing the blazar spectrum, the peak frequency  $\nu_{\text{sync}}$  of the synchrotron emission, the peak frequency  $\nu_{\text{compt}}$  of the inverse Compton emission, the total nonthermal luminosity  $L$ , the approximate ratio  $\eta$  of the total flux in the inverse Compton part to that in the synchrotron part of the spectrum, the break frequency  $\nu_{\text{break}}$ ,

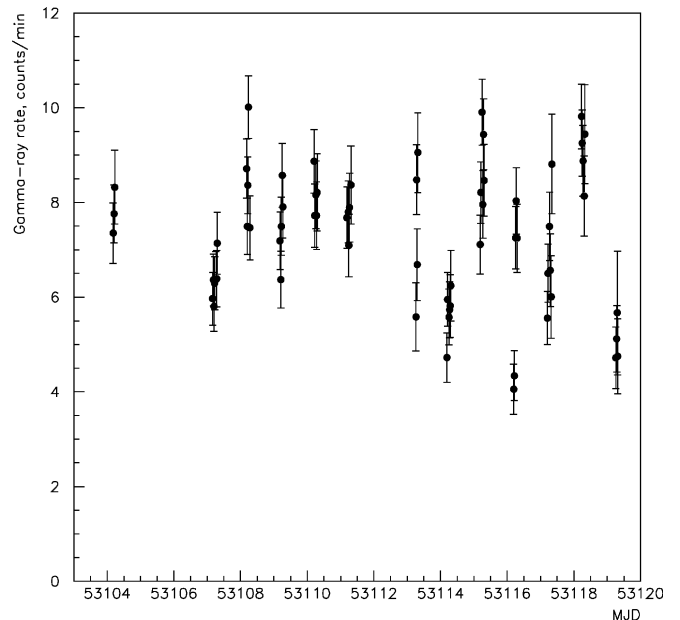


FIG. 2.—Light curve of TeV  $\gamma$ -ray emission from Mrk 421 during its outburst in 2004 April.

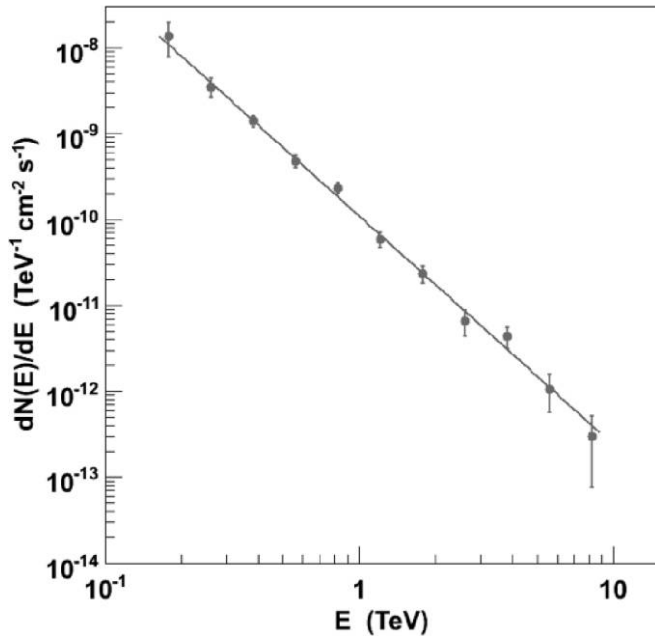


FIG. 3.—Energy spectrum of Mrk 421 measured in a high emission state during the outburst in 2004 April.

the low-frequency spectral index, and finally the fastest variability timescale  $t_{\text{var}}$ . These observables enable one to find reasonable starting values of the seven parameters of the SSC model. Using this approach we tried to fit the measured spectral energy distribution for a high state of Mrk 421. Despite the X-ray spectra being reasonably well reproduced by the one-zone SSC model, it does not provide a satisfactory fit to the TeV  $\gamma$ -ray spectrum of Mrk 421 measured in a high emission state (see Fig. 4). It is worth noting that unfolding the TeV  $\gamma$ -ray spectrum from the IR absorption (see Konopelko et al. 2003 for further details) yields an energy spectrum substantially harder than the measured one, which is more difficult to interpret in the framework of the one-zone SSC model.

## 7. DISCUSSION

Observations of Mrk 421 with Whipple (Krennrich et al. 2002) and HEGRA (Aharonian et al. 2002) during its historical flare in 2000 and 2001 have been used to extract the energy spectrum at high energies, up to 20 TeV. As stated by both groups, the energy spectrum of Mrk 421 is evidently curved.

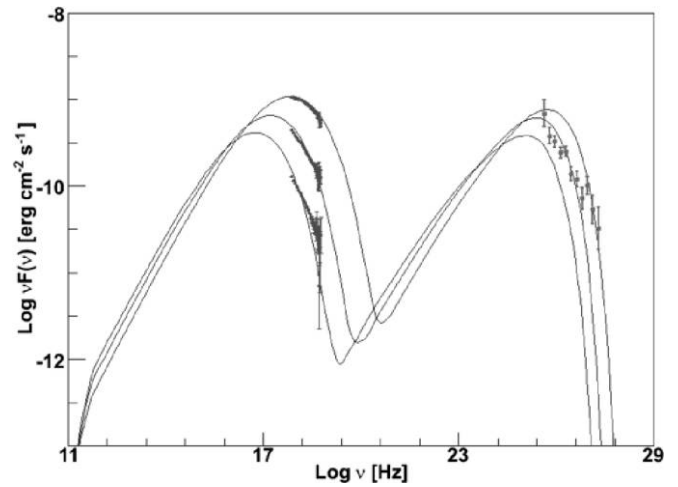


FIG. 4.—Spectral energy distribution of the Mrk 421 emission. The X-ray data, corresponding to low, medium, and high emission states, have been taken from Blazejowski et al. (2005). [See the electronic edition of the Journal for a color version of this figure.]

Analysis of the data revealed significant variations of the spectral slope at energies below 3 TeV depending on the emission state. However, the best empirical fit to the data taken in both the high and the low states gives the same cutoff energy of about 3.6 TeV. Recently, the gradual steepening in the Mrk 421 TeV energy spectrum was evidently detected with H.E.S.S. (Aharonian et al. 2005) and MAGIC (Albert et al. 2007) during their 2004 and 2005 observational campaigns. This is consistent with the assumption that all Mrk 421 spectra are affected by intergalactic absorption. Here we report on the TeV  $\gamma$ -ray spectrum as measured with the Whipple 10 m telescope during a high emission state (at the flux level of 3 crab), which does not indicate a cutoff feature in the multi-TeV energy range and can be well fitted by a pure power law. Such an unusual spectrum indicates that the curvature could be an intrinsic feature of the source. This spectrum offers a challenge for the one-zone SSC model, and it may severely constrain the spectral energy distribution of extragalactic background light, which is the subject of a forthcoming paper.

This research is supported by grants from the Smithsonian Institution, DOE (US), NSF (US), PPARC (UK), NSERC (Canada), and SFI (Ireland).

## REFERENCES

- Aharonian, F., et al. 2002, *A&A*, 393, 89  
 ———, 2005, *A&A*, 437, 95  
 Albert, J., et al. 2007, *ApJ*, 663, 125  
 Blazejowski, H., et al. 2005, *ApJ*, 630, 130  
 Davies, J., & Cotton, E. 1957, *J. Solar Energy*, 1, 16  
 Finley, J. P., et al. 2001, *Proc. 27th Int. Cosmic Ray Conf. (Hamburg)*, 7, 2827  
 Gaidos, J., et al. 1996, *Nature*, 383, 319  
 Kertzmann, M., & Sembroski, G. 1994, *Nucl. Instrum. Methods Phys. Res. A*, 343, 629  
 Kildea, J., et al. 2008, *Astropart. Phys.*, in press  
 Konopelko, A., et al. 2003, *ApJ*, 597, 851  
 Krawczynski, H., et al. 2001, *ApJ*, 559, 187  
 Krennrich, F., et al. 2002, *ApJ*, 575, L9  
 Lessard, R., et al. 2001, *Astropart. Phys.*, 15, 1  
 Mastichiadis, A., & Kirk, J. 1997, *A&A*, 320, 19  
 Mohanty, G., et al. 1998, *Astropart. Phys.*, 9, 15  
 Reynolds, P. T., et al. 1993, *ApJ*, 404, 206